Time Series Phase Unwrapping Based on Graph Theory and Compressed Sensing

Zhangfeng Ma[1], Mi Jiang[2], Mostafa Khoshmanesh[3], and Xiao Cheng[4]

[1]Hohai University
[2]Sun Yat-Sen University
[3]California Institute of Technology
[4]School of Geospatial Engineering and Science, Sun Yat-Sen University

November 24, 2022

Abstract

We present a new time series PU approach to improve the unwrapping accuracy in this article. The rationale behind is to first improve the sparse unwrapping by mitigating the phase gradient in a 2D network and then correcting the unwrapping errors in time based on the triplet phase closure. Rather than commonly-used Delaunay network, we employ All-Pairs-Shortest-Path (APSP) algorithm in graph theory to maximize the temporal coherence of all edges and to approach the phase continuity assumption in the 2D spatial domain. Next, we formulate the PU error correction in the 1D temporal domain as a compressed sensing (CS) problem, according to the sparsity rule of remaining phase ambiguity cycles. We finally estimate phase ambiguity cycles by means of Integer Linear Programming. The comprehensive comparisons on synthetic and real Sentinel-1 data covering Lost Hills, California confirm the validity of the proposed 2D+1D unwrapping approach.

Time Series Phase Unwrapping Based on Graph Theory and Compressed Sensing

Zhang-Feng Ma[1], Mi Jiang[2], Mostafa Khoshmanesh[3], Xiao Cheng[2]

[1]School of Earth Sciences and Engineering, Hohai University.

[2] School of Geospatial Engineering and Science, Sun Yat-Sen University.

[3]Department of Mechanical and Civil Engineering, California Institute of Technology.

Corresponding author: Mi Jiang

Key Points:

- We introduce an All-Pairs-Shortest-Path (APSP) algorithm in graph theory to sparse spatial phase unwrapping.
- We present an automatic unwrapping error correction method based on compressed sensing.
- The proposed correction method can correct the unwrapping error nearly 100 % under a certain condition.

Abstract

We present a new time series PU approach to improve the unwrapping accuracy in this article. The rationale behind is to first improve the sparse unwrapping by mitigating the phase gradient in a 2D network and then correcting the unwrapping errors in time based on the triplet phase closure. Rather than commonly-used Delaunay network, we employ All-Pairs-Shortest-Path (APSP) algorithm in graph theory to maximize the temporal coherence of all edges and to approach the phase continuity assumption in the 2D spatial domain. Next, we formulate the PU error correction in the 1D temporal domain as a compressed sensing (CS) problem, according to the sparsity rule of remaining phase ambiguity cycles. We finally estimate phase ambiguity cycles by means of Integer Linear Programming. The comprehensive comparisons on synthetic and real Sentinel-1 data covering Lost Hills, California confirm the validity of the proposed 2D+1D unwrapping approach.

Plain Language Summary

The PU errors can degrade performance of Time Series InSAR. Although the state-of-the-art techniques can suppress PU errors with varying degrees, the appearance of mis-estimation cannot be avoided generally. To further improve phase unwrapping accuracy, we proposed a 2-step 3-D PU approach. Different from conventional 3-D unwrapping that first estimates spatial phase difference on edge in regular grid or in Delaunay triangle, we maximize the quality of Delaunay network by means of APSP (All-Pairs-Shortest-Path) algorithm under the framework of graph theory, in which the bad edges are substituted with the better edges. In the second step, we calculate the closure phase triplets to check the unwrapping error, and Integer Linear Programming we borrowed from Compressed Sensing is used to automatic correct the PU errors. We found ILP can correct almost all the PU errors when the number of interferograms with PU errors is less than half the number of triangle loops in SBAS graph.

1 Introduction

The aim of Phase Unwrapping (PU) is to recover the proper ambiguity number of the phase cycle 2π from the interferogram, in which the observations are known modulo-2π [*Hussain et al.*, 2016; *Yu et al.*, 2019]. In order to identify the ambiguous phase cycles, a prior phase continuity assumption that the local phase gradient between neighboring points should be less than π makes this problem tractable. Based on this concept, the 1D+2D method presented by Pepe and Lanari [*Pepe and Lanari*, 2006] integrates the temporal MCF network programming with the spatial PU to mitigate phase gradients (local topography and atmospheric turbulence) and therefore approach the phase continuity assumption. In 3D-based methods, the phase continuity assumption is extended to three dimensions. Costantini [*Costantini et al.*, 2012] first proposed a multi-dimensional PU procedure, in which redundant phase gradients both in temporal and spatial dimensions are utilized in optimizing 3D irrotationality constraints. Hooper and Zebker [*Hooper and Zebker*, 2007] proposed a QUASI-L∞-Norm 3D PU algorithm, which extends the 2D branch-cut theory to 3D through linking phase residuals to construct a 3D discontinuity surface. Although these 3D PU approaches are likely to achieve reliable results, heavy computational burden and the error propagation induced by violating the phase continuity may degrade the unwrapping efficiency.

Recent studies have demonstrated that the phase error correction is a powerful compensation after PU [*Biggs et al.*, 2007]. After establishing a linear relationship between triplet phase closure and

unwrapped phase observations (see 2.2), a correction operator is implemented pixel by pixel to compensate PU errors [*Fattahi*, 2015; *Xu and Sandwell*, 2020]. In this context, here we reformulate this problem of integer ambiguity correction under the mathematical framework of compressed sensing (CS) technique and replace the nonconvex discontinuous L0-Norm by the convex continuous L1-Norm, leading to an L1-Norm integer linear programming (ILP). We also investigate the 2D PU on the sparse grid, with emphasis on the spatial reference network. As a result, time series PU becomes the focus of this study.

2 Method

2.1 Sparse PU Based on APSP Algorithm

In Sparse PU (SPU), the Delaunay triangulation is a commonly-used method to connect all sparse points. However, the algorithm seeks whether the convex hull of neighboring two triangles contains other points and whether triangles overlap, and is independent of the rule of phase continuity. This implies many edges may have higher phase difference in a spatial network when deformation signals, atmospheric turbulence, and phase noise are present in the interferogram. The temporal coherence is a valid measure to quantify the phase difference:

$$\rho = \frac{1}{M}\left|\sum_{i=1}^{M} e^{j\Delta\phi_{i,p,q}}\right| \tag{1}$$

where $\Delta\phi_{i,p,q}$ is the phase difference between vertex p and q in an interferogram i. The higher values of temporal coherence represents that an edge has a smaller phase variation in the temporal dimension. Accordingly, it is favorable to select edges with higher temporal coherence to improve the unwrapping results for all the interferograms, instead of using the edges obtained from the Delaunay triangulation algorithm. To this end, the All-Pairs-Shortest-Path (APSP) algorithm can be updated the edge set (Text S1). Once all edges are updated using the APSP algorithm, the total temporal coherence of the newly generated network is maximized. Given such an APSP network, MCF algorithm can be implemented to obtain the phase ambiguities. Nevertheless, here we use a slightly different form of the MCF, based on triangle irrotationality constraint for Delaunay triangulations.

For a Delaunay network of M triangles and N edges, the MCF objective function is formulated as:

$$\begin{gathered}\left[A_{M\times N} \quad -A_{M\times N}\right]\begin{bmatrix}K^{+}_{N\times 1}\\ K^{-}_{N\times 1}\end{bmatrix} = U_{M\times 1}\\ \arg\min\left\{f^{+}_{1\times N}K^{+}_{N\times 1} + f^{-}_{1\times N}K^{-}_{N\times 1}\right\}\ .\\ K^{+},K^{-}\in\mathbb{N}^{0}\end{gathered} \tag{2}$$

In (2), K^{+} and K^{-} are two slack vectors for edge ambiguities to be computed, f^{+} and f^{-} are probability cost for those two slack vectors, and A is the design matrix, which is determined by all triangles in Delaunay, defined as

$$A_{M\times N}=\begin{bmatrix} a_{11} & a_{12} & a_{13} & \cdots & a_{1N} \\ a_{21} & a_{22} & a_{23} & \cdots & a_{2N} \\ \vdots & \vdots & \vdots & \vdots & \vdots \\ a_{M1} & a_{M2} & a_{M3} & \cdots & a_{MN} \end{bmatrix}$$
$$\text{s.t.} a_{ij}=\begin{cases} -1, \text{if } E_j \text{ is counter-clockwise direction in } Tri_i \\ 1, \text{ if } E_j \text{ is clockwise direction in } Tri_i \\ 0, \text{ otherwise} \end{cases} . \quad (3)$$
$$(i=1,2,3,...,M;\ j=1,2,3,...,N)$$

The triangle irrotationality constraint U is defined as follows:

$$U_i=\sum_{j=1}^{N} a_{ij}\cdot n_j$$
$$\text{s.t. } n_j=round(-\delta\phi_j/2\pi) \quad (4)$$

where $\delta\phi_j$ is the phase difference of E_j. When an optimal solution of K^+ and K^- is found, ambiguities for all edges are calculated by K^+-K^-. Next, the ambiguities estimated for connected edges are integrated through flood-fill procedure to determine the ambiguity cycles of all points.

It is worth noting that some triangles are eliminated after APSP, which makes the triangle irrotationality constraint infeasible. We solve this issue by converting the constraint from the triangle to the edge, using the edgelist phase unwrapping algorithm presented in [*Shanker and Zebker*, 2010]. More specifically, for an APSP network with N edges and P points, the MCF objective function is defined as:

$$\begin{bmatrix} A_{N\times P} & -A_{N\times P} & I_{N\times N} & -I_{N\times N} \end{bmatrix}\begin{bmatrix} m^+_{P\times 1} \\ m^-_{P\times 1} \\ K^+_{N\times 1} \\ K^-_{N\times 1} \end{bmatrix}=S_{N\times 1}$$
$$\arg\min\left\{ f^+_{1\times N}K^+_{N\times 1}+f^-_{1\times N}K^-_{N\times 1}\right\} \quad (5)$$
$$m^+,m^-,K^+,K^-\in\mathbb{N}^0$$

where I is the unit matrix, m^+ and m^- are two slack vectors for point ambiguities, and A is the design matrix defined as

$$A_{N\times P}=\begin{bmatrix} a_{11} & a_{12} & a_{13} & \cdots & a_{1P} \\ a_{21} & a_{22} & a_{23} & \cdots & a_{2P} \\ \vdots & \vdots & \vdots & \vdots & \vdots \\ a_{N1} & a_{N2} & a_{N3} & \cdots & a_{NP} \end{bmatrix}$$
$$\text{s.t.} a_{ij}=\begin{cases} 1, \text{if j is starting node in } E_i \\ -1, \text{ if j is destination node in } E_i \\ 0, \text{ otherwise} \end{cases} . \quad (6)$$
$$(i=1,2,3,...,N;\ j=1,2,3,...,P)$$

Moreover, the edge constraint S of E_i is defined as $S_i=round(-\delta\phi_i/2\pi)$ where $\delta\phi_i$ is the phase difference of E_i. When the MCF method obtains the optimal solution using (5), point ambiguities are estimated by m^+-m^- and, hence, the flood-fill operation is not required. It, therefore, reduces the computational burden for the PU process.

In summary, APSP-Based SPU is composed of three steps: (1) generation of the Delaunay triangulation, (2) forming the APSP network based on the temporal coherence, and (3) retrieval of the phase ambiguities on all the sparse points using the edgelist phase unwrapping algorithm.

2.2 Phase Unwrapping Error Correction Using CS

2.2.1 Phase Ambiguity Correction

Given a triangle loop of three unwrapped phases $\psi_{m,j}$, $\psi_{j,k}$ and $\psi_{m,k}$ obtained from interference of three acquisitions *m*, *j* and *k*, the phase closure $\Delta\psi_{m,j,k}$ is defined as [*Biggs et al.*, 2007; *Xu and Sandwell*, 2020]

$$\Delta\psi_{m,j,k} = \psi_{m,j} + \psi_{j,k} - \psi_{m,k} \quad . \tag{7}$$

The non-zero $\Delta\psi_{m,j,k}$ represents errors, which may be caused by the decorrelation noise, multi-looking, filtering, and/or PU errors. Assuming PU errors as the sole cause of non-zero $\Delta\psi_{m,j,k}$, he residual phase ambiguity in the triangle loop is expressed as $U_{m,j,k} = round(-\Delta\psi_{m,j,k} / 2\pi)$ [*Fattahi*, 2015; *Yunjun et al.*, 2019]

$$U_{m,j,k} = round(-\Delta\psi_{m,j,k} / 2\pi) \tag{8}$$

Based on the concept of phase closure, an L^2-Norm [*Fattahi*, 2015] and a LASSO [*Park and Casella*, 2008; *Xu and Sandwell*, 2020] method were proposed to handle the PU errors. Their objective functions are respectively defined as

$$\begin{aligned} &\arg\min\left\{\left\|GX - U\right\|_2\right\} \\ &\arg\min\left\{\left\|AX - U\right\|_2 + \alpha\left\|X\right\|_1\right\} \end{aligned} \quad . \tag{9}$$

where *G* is the incidence matrix of L2-Norm method, *A* is the incidence matrix of LASSO method and α is the Lagrange multiplier. *X* and *U* are ambiguity vector and phase closure, respectively. Details of the construction of *G* and *A* matrices are described in Text .S2.

Limited to the global smoothness of L2-Norm, the above mentioned two methods both need a risky round operator to obtain the integer solutions. To illustrate, 0.5 would be rounded to 1. Moreover for LASSO, the parameterization and selection of α is time-consuming.

2.2 Compressed Sensing and Integer Linear Programming

Here we propose to solve the error correction problem based on the CS framework. Compared to the conventional recovery techniques [*Fowler*, 2009; *Jain*, 1981], CS [*Candes and Tao*, 2005; 2006; *Duarte and Eldar*, 2011; *Gribonval and Nielsen*, 2003] seeks to recover signals from fewer samples than those required by the Nyquist rate. This issue can be effectively resolved only if: 1) solutions are sparse and $k < Spark(A)/2$, where *k* is the number of non-zero elements in the solution vector and *Spark* denotes the smallest rank of columns and rows; 2) the incidence matrix *A* fulfills the Restricted Isometry Property (RIP) condition [*Candes and Tao*, 2005], meaning the incidence matrix and its transform base should be incoherent. It is still an elusive topic in information theory to determine which ensembles can satisfy the RIP condition with high probability.

In the case of redundant SBAS graph, however, it is possible to check whether the incidence matrix meets the aforementioned criteria[*Zhao et al.*, 2018]. The *Spark* of *A* is *T* (the number of triangle

loop in SBAS graph) [*Murty, 2017a; b*], and therefore the sparsity must follow $k < T/2$. Otherwise, the signal recovery degree will be greatly affected. It is reasonable to assume that some pixels in the interferograms contain no PU errors, and phase ambiguity of those pixels are zero. In this case, compressed sensing can be used to recover the phase ambiguity. For every *k*-sparse solution vector, *X* is the unique solution to the L^0 optimization criterion

$$\begin{aligned} &\arg\min \|X\|_0 . \\ &s.t. AX = U \end{aligned} \tag{10}$$

However, (10) cannot be solved in a polynomial time [26]. To overcome this challenge, a common strategy that converts (10) to a convex optimization based on L^1-Norm is given by [27]

$$\begin{aligned} &\arg\min \left\| f^T X \right\|_1 \\ &s.t. AX = U \end{aligned} \tag{11}$$

where f^T is the reciprocal of the coherence vector, and (11) can be treated as a linear programming (LP) problem. Given the integer property of solutions, an integer linear programming (ILP) method based on LP is proposed to solve (11), which can directly obtain the integer solution, while (9) can only obtain the non-integer solutions.

In this study, we follow the basic concepts of L^1-Norm. The overall features our proposed approach is compared with other methods in Table.S1. Notably, obtaining integer solution for phase ambiguity correction problem, to the best of our knowledge, is proposed and discussed for the first time in this study.

Before searching for an ILP solution, we need to reformulate the objective function of L^1-Norm for phase ambiguity correction, (11), in a way that all the parameters to be estimated are non-negative. In order to do this, we introduce two slack vectors X^+ and X^- for phase ambiguity *X*. Rewriting (11) in terms of these slack vectors into

$$\begin{aligned} &\begin{bmatrix} A & -A \end{bmatrix} \begin{bmatrix} X^+ \\ X^- \end{bmatrix} = U \\ &X^+, X^- \in \mathbb{N}^0; X^+, X^- \le l_{up} \end{aligned} \tag{12}$$

with

$$\arg\min \left\| f^T (X^+ - X^-) \right\|_1 \tag{13}$$

where l_{up} is the upper boundary of the solutions.

It is a difficult task to solve (13) given the extreme computational complexity of ILP. GUROBI optimization, which incorporates Branch-and-Cut (BC), heuristic and parallelism techniques is used to complete the solving process of (12-13) [*Ladányi et al.*, 2001]. In particular, the subroutine "intlinprog.m" in GUROBI has been used as the ILP solver.

3 Synthetic Data Test

3.1 Performance of APSP Network in Spatial PU

Simulated observations provide a great opportunity for testing the performance of APSP and comparison with other 2D SPU methods, as the true values are available. Our synthetic observation consists of 10,000 sparse points, randomly distributed in a rectangle of size 2000×2000 (Fig.1a).

50 interferorgams are simulated by randomly generated temporal and perpendicular baselines. The linear deformation rate is simulated by peaks function of MATLAB, shown in Fig.1a. The simulated phase of the atmospheric and noise components of the 50^{th} interferogram are shown in Fig.1b and Fig.1c, respectively. In addition, the phase noise is simulated by γ=0.3 [*Hanssen*, 2001]. Fig.1d shows the 50^{th} simulated interferogram containing deformation, atmospheric, and noise elements. In this experiment, we compare the APSP-Based SPU with the original SPU based on MCF.

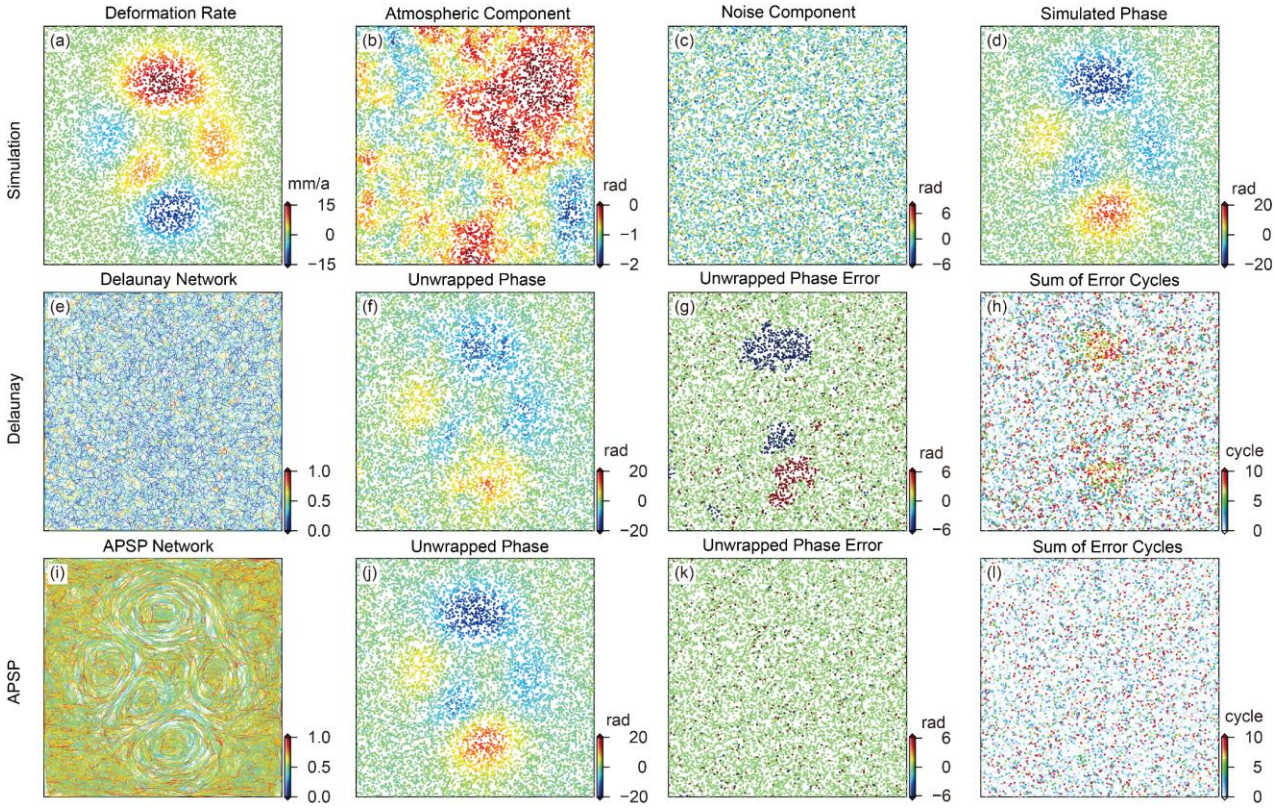

Figure 1. (a) Simulated deformation rate. (b) Simulated atmospheric phase component of the 50th interferogram (c) Simulated noise phase component of the 50th interferogram (d) The 50th simulated interferogram. (e-h) are the results obtained from Delaunay network: (e) temporal coherence, (f) unwrapped phase, (g) unwrapped phase errors, and (h) the sum of absolute ambiguity cycles in 50 interferograms. Similarly, (i-l) are results of APSP network.

First, we investigate the performance of APSP algorithm in updating the Delaunay. Comparing Fig.1i with Fig.1e, the temporal coherence of the edges has improved significantly by using the APSP. Moreover, the unwrapped phase resulting from implementing these two approaches (Fig.1f and 1j) show notable differences. In particular, the unwrapping errors are significantly lower in the results obtained from APSP method (Fig.1k) when compared to that from MCF based on the Delaunay triangulation (Fig.1g). Errors mainly occur where the deformation gradients are large. Therefore, reduction of the unwrapping errors shows that the updated APSP network, which considers phase differences through introducing temporal coherence can more easily satisfy the phase continuity assumption. Lastly, we compare the sum of absolute values of the ambiguity integer cycles in 50 interferograms. One ambiguity integer cycle means an unwrapping error of

2π. Results of APSP in Fig.1l indicate a higher accuracy than that of Delaunay in Fig.1h especially in the high deformation gradient regions.

Using the simulated interferograms, we conducted a statistical test to evaluate how much PU errors are reduced through APSP. In this statistical test, the coherence is set to different values ranging from 0.05 to 0.95. The simulation is repeated 1000 times and the percentages of points containing PU error are recorded in each simulation. The averaged results are shown in Fig.S1. In most coherence cases, PU errors of APSP are about half of that from Delaunay, which further shows the effectiveness of APSP for reducing PU errors in the spatial domain.

3.2 Performance of ILP in PU Ambiguity Correction

To validate the phase ambiguity correction using ILP, a Monte-Carlo test is carried out. The simulated SBAS pairs and their associated spatiotemporal baselines are shown in Fig.3b, following [*Xu and Sandwell*, 2020]. The phase components consist of a linear trend of 50 mm/a, a seasonal signal with the amplitude of 20 mm and a noise component with standard deviation of 10 mm. In addition to these three components, ±4π phase ambiguities are randomly added to different percentages of the SBAS interferograms. This Monte-Carlo experiment is repeated 8000 times. Fig.2a shows the statistical results.

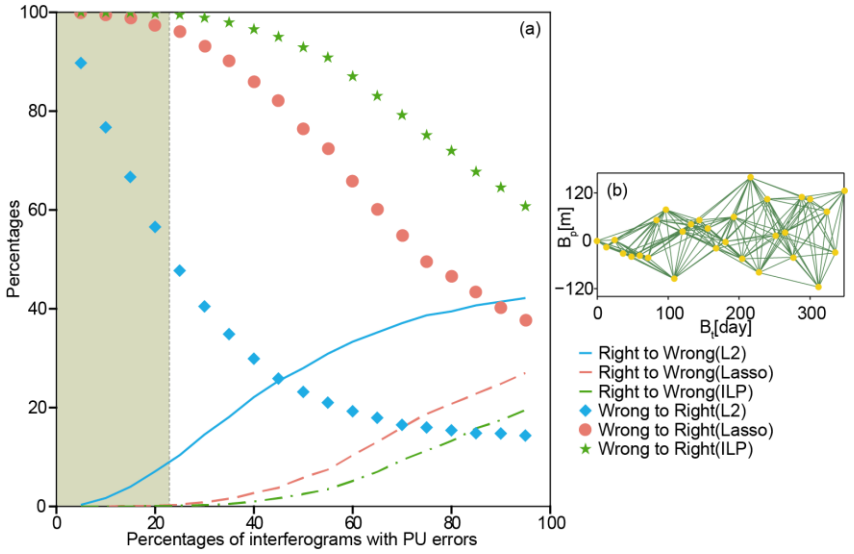

Figure 2. Statistical results of three methods in phase ambiguity correction and simulated TP plane in the test. (a) The statistical results, and (b) the simulated TP plane.

In this test, the three PU methods are evaluated from two different aspects: 1) how many interferograms with PU errors are corrected ("Wrong to Right"); 2) how many interferograms without PU errors are unwrapped incorrectly ("Right to Wrong"). It can be seen from Fig. 2a that L2 is the least effective correction method with highest percentage of "Right to Wrong" across different percentages of interferograms with PU error introduced. The Lasso solver achieves a better result compared to the L2 in terms of both percentage of corrected and the "Right to Wrong" interferograms. ILP solver, on the other hand, achieves the best results compared to both the L2 and Lasso solvers, regardless of the percentage of interferograms with PU errors. The test results also show that ILP corrects almost all the PU errors when the number of interferograms with PU errors is less than half the number of triangular loops in SBAS interferograms. This region is

highlighted with a green rectangle in Fig. 2a for this simulation. This is mainly due to the fact that the sparsity of $\left[X^{+} \quad X^{-}\right]^{T}$ in this region is less than $spark([A \quad -A])/2$, as mentioned in Section 2.2. Although the accuracy of ILP decreases when the number of interferograms with PU errors exceed this threshold, its performance is still superior to the other two methods. Also, the APSP network can provide a SPU results with less PU errors. Therefore, the integration of APSP in SPU and ILP in temporal correction can make the final PU results more reliable.

4 Real Data Test

A stack of Sentinel-1 TOPS images over Lost Hills in south California is chosen as the test data. The data set includes 57 SLCs during January 2017 to November 2018, acquired from a descending orbit. The temporal network we used in this experiment is the sequential network [*Fattahi et al.*, 2016], in which the neighboring 4 acquisitions of each acquisition are interconnected.

4.1 Performance of APSP Network

To highlight the performance of APSP, Fig.3 presents a comparison between unwrapped interferorgams based on Delaunay and APSP. It can be clearly seen that points in isolated regions of farmland (inside dashed rectangle of Fig.3) are clearly unwrapped incorrectly, while the results associated with APSP network (Fig. 3b) are almost error-free.

To further investigate the effectiveness of APSP network, the number of non-closing triplets in unwrapped interferorgams is shown in Fig.3c-d. The smaller the proportion of the non-closing triplets in the total number of interferogram triplets, the higher the reliability of the unwrapped results.

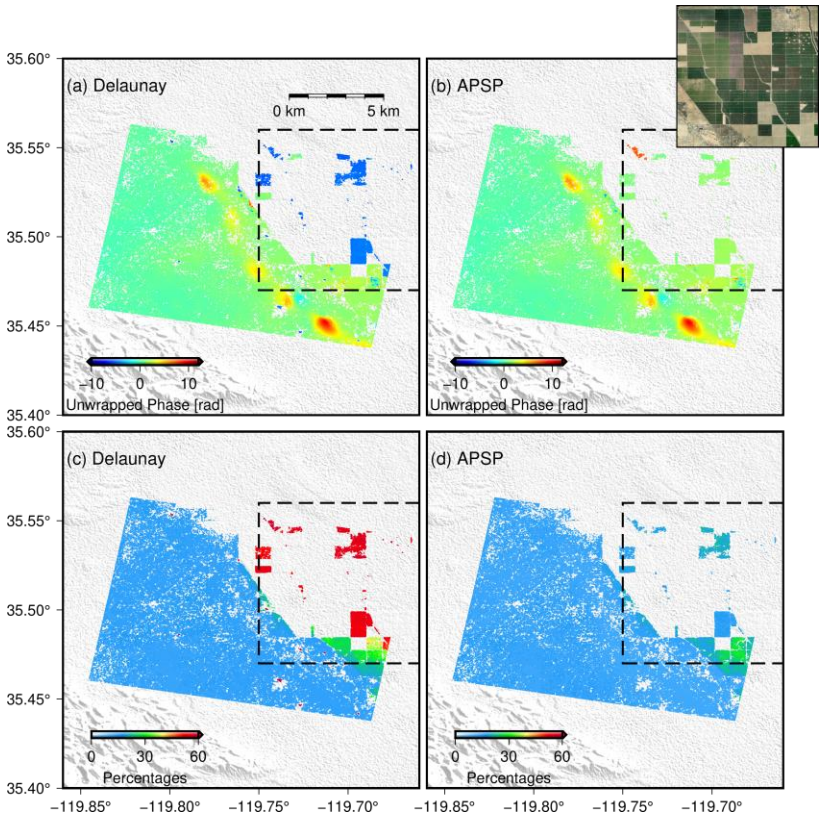

Figure 3. Unwrapped Interferograms (20180806-20180830) based on different networks and percentages of non-closing loops in all interferogram triplets. (a) and (b) are respectively the unwrapped Interferogram of Delaunay network and APSP network. (c) and (d) are percentages of non-closing loops in all interferogram triplets respectively.

It can be seen in Fig.3c-d that the non-closing loops in the results obtained from Delaunay by far exceed that of APSP network, indicating the superior performance of the APSP. Moreover, since only the networks are different in the PU process, we expect to see further improvement in the PU results by incorporating SPU. As shown in the simulation test (Fig.2a), lower spatial unwrapping errors would be beneficial in the temporal correction step using every phase ambiguity correction methods discussed in this study.

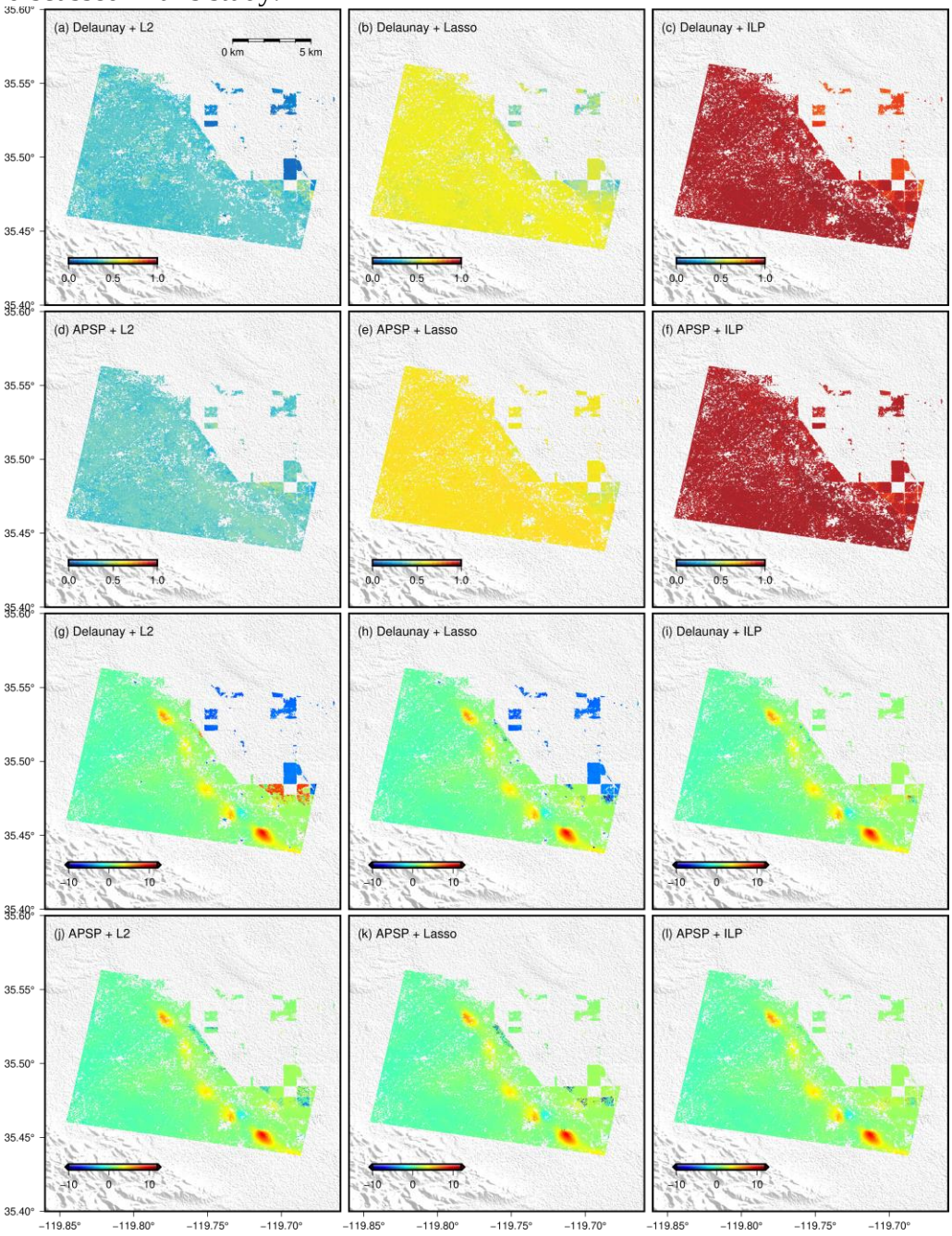

Figure 4. Temporal coherence of all interferograms after correction and corrected interferograms (20180806-20180830) of three methods based on different networks. (a-e) are respectively the temporal coherence of Delaunay and L2, Delaunay and Lasso, Delaunay and ILP, APSP and L2, APSP and Lasso, APSP and ILP method. (g-l) are unwrapped interferograms of them.

4.2 Performance of ILP in Phase Ambiguity Correction

To highlight the ILP's performance in correcting phase ambiguity, Fig.S2 presents a comparison of uncorrected proportions for all the interferogram triplets between different solvers. The percentage of non-closing triplets by using the Delaunay is larger than that based on APSP, regardless of the PU error correction method. Using the Delaunay, error percentages of ILP is centered at ~1%, while L2 and Lasso are at 11% and 3%, respectively. However, using the ASPS further reduces error percentages to near zero for ILP, and down to 2% and 8% for the results obtained from Lasso and L2, respectively.

To quantitatively demonstrate the effect of ambiguity correction methods, we calculate the temporal coherence γ for each pixel, by replacing the wrapped phases with the unwrapped result in (1) as:

$$\gamma=\frac{1}{M}\left|\sum_{i=1}^{M}e^{j(\psi_i-\hat{\psi}_i)}\right| \qquad (14)$$

where $\hat{\psi}$ is the unwrapped phase of interferogram $i=1,\ldots,M$.

Since the SBAS network of interferograms is fully connected, the remaining unwrapping errors can be considered as the principle source of noise compared to the magnitude of decorrelation noise. With this assumption, $\gamma=1$ indicate no remaining unwrapping errors in the interferogram set, while $\gamma<1$ implies the occurrence of uncorrected phase ambiguity.

Fig. 4a-c respectively show the temporal coherence of the three temporal correction methods after spatial ambiguity correction using Delaunay triangulation. Fig.4d-f demonstrate the associated results by using the APSP network. As expected from Fig. 3a, the coherence map associated with the results obtained from APSP network are overall higher than that of Delaunay triangulation. This is mainly resulting from the effectiveness of APSP network in reducing spatial PU errors. Moreover, the coherence maps by using ILP results in values close to 1 in both APSP and Delaunay. Whereas, the maximum coherence of L2 and Lasso are close to 0.4 and 0.7. The superior performance of ILP results is expected from our simulation test (Fig. 2a).

For further validation of the performance of ILP, several corrected interferograms are presented in Fig.4g-i for visual inspection. It can be seen that, regardless of the choice of the networking method used, the isolated regions with unwrapping errors are mostly corrected by using the ILP solver (Fig. 4i&l). In the results based on Delaunay triangulation (Fig. 4g&j), L2 and Lasso failed to correct those unwrapping errors. For the results based on APSP network (Fig.4h&k), although Lasso corrected most of the unwrapping errors, it still failed to correct the errors in some very small areas. These results further validate the performance of our proposed 2D+1D framework.

4.3 Processing Time

For APSP, an additional time is required to search for the shortest paths between all the initial edges provided by the Delaunay triangulation. This is the most time-consuming step in our method. With a Matlab 2018b software and an Intel i7 3.2GHz processor, the generation of APSP network for 259361 sparse points takes 3452s. However, in the following PU step in spatial domain, APSP

network consisting of 781075 edges takes less time than Delaunay network with 776399 edges. APSP network operates 9892s to solve ILP solutions for 218 interferograms, while Delaunay network takes 10738s. This is because there are more reliable edges in the APSP network, which are less likely to have phase ambiguities required to be compensated for. Therefore, it directly helps to reduce the total objective function cost. Subplot in Fig.S4 shows the APSP and Delaunay objective cost of 218 interferograms when exiting the ILP process. APSP outperforms Delaunay in objective cost and time consuming for most of interferograms. Also, we present the iteration process and its relative computing time of the interferogram for 20180806-20180830 as an example. In iteration, total cost and computing time of APSP are all less than that of Delaunay.

It is important to note that the part of time cost reduction comes from the edge constraint introduced in Section 2.1. In the original SPU, phase cycles of all edges are required to integrate to each point using flood fill. This integration process was abandoned in this paper because it needs a long time to complete the integration for all interferograms. The modifications to the MCF objective function can help to directly obtain the phase ambiguity of all sparse points so as to improve the computational efficiency.

In temporal correction using different methods, L2 and ILP solver have shown their great efficiency. L2 takes 1210s to finish the phase ambiguity correction, and ILP takes 1265s. However, for finishing the phase ambiguity correction, Lasso consumes a very long time up to 81354s. We therefore can conclude our proposed method can achieve high accuracy in an efficient manner.

5 Conclusions

In this paper, a 3D (2D + 1D) PU method has been presented that integrates the APSP network on spatial domain with ILP on temporal domain. First, the APSP network has been proposed to replace the Delaunay network in the spatial domain. The temporal coherence of edges are treated as the edge length function. APSP algorithm is used to maximize the temporal coherence of edges between two points. Thus, the phase difference induced by deformation and noise are reduced, making it easier to satisfy the phase continuity assumption. In addition, ILP based on CS framework is first introduced in this paper for phase ambiguity correction in the temporal domain. In addition to the great performance in terms of accuracy, another main advantage of this method is that it only modifies integer phase ambiguities without the change of the fractional part of the unwrapped phase. The effectiveness of the implemented integration of APSP network and ILP has been demonstrated on both synthetic data and a set of Sentinel-1 TOPS interferograms over Lost Hills, CA region. Based on these validation analysis, we conclude that the proposed 3D PU method can make time series PU more accurate.

Acknowledgments and Data

Sentinel-1 data were freely provided by the European Space Agency (https://scihub.copernicus.eu/). Some figures were drawn by Generic Mapping Tools 6.1.0 software ([*Wessel et al.*, 2019]). The authors thank GUROBI company for providing the academic license of GUROBI software (License ID: 413287, https://www.gurobi.com/free-trial/). The APSP network based spatial PU and compressed sensing based PU error correction here described are a MATLAB-based application developed by us (https://sites.google.com/view/mazhangfeng). This work was supported in part by the National Natural Science Foundation of China under Grant 41774003 and 42074008, and in part by the ESA-MOST Dragon 5 project under Grant 59332.

References

Biggs, J., T. Wright, Z. Lu, and B. Parsons (2007), Multi-interferogram method for measuring interseismic deformation: Denali Fault, Alaska, *Geophysical Journal International*, *170*(3), 1165-1179.
Candes, E. J., and T. Tao (2005), Decoding by linear programming, *IEEE Transactions on Information Theory*, *51*(12), 4203-4215.
Candes, E. J., and T. Tao (2006), Near-Optimal Signal Recovery From Random Projections: Universal Encoding Strategies?, *IEEE Transactions on Information Theory*, *52*(12), 5406-5425.
Costantini, M., F. Malvarosa, and F. Minati (2012), A General Formulation for Redundant Integration of Finite Differences and Phase Unwrapping on a Sparse Multidimensional Domain, *IEEE Transactions on Geoscience and Remote Sensing*, *50*(3), 758-768.
Duarte, M. F., and Y. C. Eldar (2011), Structured Compressed Sensing: From Theory to Applications, *IEEE Transactions on Signal Processing*, *59*(9), 4053-4085.
Fattahi, H. (2015), Geodetic imaging of tectonic deformation with InSAR, Ph.D. thesis, 190 pp, University of Miami, Ann Arbor.
Fattahi, H., P. Agram, and M. Simons (2016), A network-based enhanced spectral diversity approach for TOPS time-series analysis, *IEEE Transactions on Geoscience and Remote Sensing*, *55*(2), 777-786.
Fowler, J. E. (2009), Compressive-Projection Principal Component Analysis, *IEEE Transactions on Image Processing*, *18*(10), 2230-2242.
Gribonval, R., and M. Nielsen (2003), Sparse representations in unions of bases, *IEEE Transactions on Information Theory*, *49*(12), 3320-3325.
Hanssen, R. F. (2001), *Radar interferometry: data interpretation and error analysis*, Springer Science & Business Media.
Hooper, A., and H. Zebker (2007), Phase unwrapping in three dimensions with application to InSAR time series, *J. Opt. Soc. Am. A*, *24*(9), 2737-2747.
Hussain, E., A. Hooper, T. J. Wright, R. J. Walters, and D. P. S. Bekaert (2016), Interseismic strain accumulation across the central North Anatolian Fault from iteratively unwrapped InSAR measurements, *Journal of Geophysical Research: Solid Earth*, *121*(12), 9000-9019.
Jain, A. K. (1981), Image data compression: A review, *Proceedings of the IEEE*, *69*(3), 349-389.
Ladányi, L., T. K. Ralphs, and L. E. Trotter (2001), Branch, Cut, and Price: Sequential and Parallel, in *Computational Combinatorial Optimization: Optimal or Provably Near-Optimal Solutions*, edited by M. Jünger and D. Naddef, pp. 223-260, Springer Berlin Heidelberg, Berlin, Heidelberg.
Murty, P. S. R. (2017a), Chapter 3 - Incidence Matrices, in *Power Systems Analysis (Second Edition)*, edited by P. S. R. Murty, pp. 19-33, Butterworth-Heinemann, Boston.
Murty, P. S. R. (2017b), Chapter 2 - Graph Theory, in *Power Systems Analysis (Second Edition)*, edited by P. S. R. Murty, pp. 7-17, Butterworth-Heinemann, Boston.
Park, T., and G. Casella (2008), The Bayesian Lasso, *Journal of the American Statistical Association*, *103*(482), 681-686.
Pepe, A., and R. Lanari (2006), On the Extension of the Minimum Cost Flow Algorithm for Phase Unwrapping of Multitemporal Differential SAR Interferograms, *IEEE Transactions on Geoscience and Remote Sensing*, *44*(9), 2374-2383.
Shanker, A. P., and H. Zebker (2010), Edgelist phase unwrapping algorithm for time series InSAR analysis, *J. Opt. Soc. Am. A*, *27*(3), 605-612.
Wessel, P., J. F. Luis, L. Uieda, R. Scharroo, F. Wobbe, W. H. F. Smith, and D. Tian (2019), The Generic Mapping Tools Version 6, *Geochemistry, Geophysics, Geosystems*, *20*(11), 5556-5564.
Xu, X., and D. T. Sandwell (2020), Toward Absolute Phase Change Recovery With InSAR: Correcting for Earth Tides and Phase Unwrapping Ambiguities, *IEEE Transactions on Geoscience and Remote Sensing*, *58*(1), 726-733.
Yu, H., Y. Lan, Z. Yuan, J. Xu, and H. Lee (2019), Phase Unwrapping in InSAR : A Review, *IEEE Geoscience and Remote Sensing Magazine*, *7*(1), 40-58.
Yunjun, Z., H. Fattahi, and F. Amelung (2019), Small baseline InSAR time series analysis: Unwrapping error correction and noise reduction, *Computers & Geosciences*, *133*, 104331.
Zhao, M., M. D. Kaba, R. Vidal, D. P. Robinson, and E. Mallada (2018), Sparse Recovery over Graph Incidence Matrices, paper presented at 2018 IEEE Conference on Decision and Control (CDC), 17-19 Dec. 2018.